

1

2 **Genomic diversity of novel strains of mammalian gut microbiome derived *Clostridium***
3 **XIVa strains is driven by mobile genetic element acquisition**

4

5 Maya T. Kamat^{a\$}, Michael J. Ormsby^{a,b\$}, Suzanne Humphrey^a, Katja Thümmler^a, Craig
6 Lapsley^a, Kathryn Crouch^a, Caitlin Jukes^a, Heather Hulme^{a,c}, Richard Burchmore^a, Lynsey M.
7 Meikle^a, Leighton Pritchard^{c,*} and Daniel M. Wall^{a,*}

8

9 ^a*School of Infection and Immunity, College of Medical, Veterinary and Life Sciences, Sir*
10 *Graeme Davies Building, University of Glasgow, Glasgow G12 8TA, United Kingdom*

11 ^b*Biological and Environmental Sciences, Faculty of Natural Sciences, University of Stirling,*
12 *Stirling, FK9 4LA, United Kingdom*

13 ^c*Strathclyde Institute of Pharmacy & Biomedical Sciences, Strathclyde University, Glasgow*
14 *G4 0RE, United Kingdom*

15 ^{\$}*Contributed equally to the work*

16

17 ^{*}*Corresponding author email addresses: Donal.Wall@glasgow.ac.uk;*

18 Leighton.Pritchard@strath.ac.uk

19

20 **Abstract**

21 Despite advances in sequencing technologies that enable a greater understanding of
22 mammalian gut microbiome composition, our ability to determine a role for individual strains
23 is hampered by our inability to isolate, culture and study such microbes. Here we describe
24 highly unusual *Clostridium* XIVa group strains isolated from the murine gut. Genome
25 sequencing indicates that these strains, *Clostridium symbiosum* LM19B and LM19R and
26 *Clostridium clostridioforme* LM41 and LM42, have significantly larger genomes than most
27 closely related strains. Genomic evidence indicates that the isolated LM41 and LM42 strains
28 diverge from most other *Clostridium* XIVa strains and supports reassignment of these groups
29 at genus-level. We attribute increased *C. clostridioforme* LM41 and LM42 genome size to
30 acquisition of mobile genetic elements including dozens of prophages, integrative elements,
31 putative group II introns and numerous transposons including 29 identical copies of the IS66
32 transposase, and a very large 192 Kb plasmid. antiSmash analysis determines a greater
33 number of biosynthetic gene clusters within LM41 and LM42 than in related strains,
34 encoding a diverse array of potential novel antimicrobial compounds. Together these strains
35 highlight the potential untapped microbial diversity that remains to be discovered within the
36 gut microbiome and indicate that, despite our ability to get a top down view of microbial
37 diversity, we remain significantly blinded to microbe capabilities at the strain level.

38

39

40

41

42

43

44

45

46

47

48 **Introduction**

49 The intestinal microbiome is now recognized as playing an important role in the
50 maintenance of human health, providing protection from invading pathogens and potentially
51 contributing to a variety of diseases when disrupted [1–6]. While significant progress has been
52 made in understanding alterations to the human gut microbiome across a range of diseases,
53 identification of a defined mechanistic role for the microbiome in many of these diseases has
54 yet to be elucidated. However, significant and reproducible alterations in the gut microbiome
55 associated with many diseases have added further weight to the suggestion that bidirectional
56 communication between the gut and various organs, including the brain, may contribute to
57 specific conditions. Microbiome-derived metabolites and microbe-modulated host
58 neurotransmitters are known to cross the blood-brain barrier [5, 7–10], and *Lachnospiraceae*-
59 derived metabolites localize to the white matter of the murine brain and inhibit energy
60 production in white matter cells when tested *ex vivo* [9]. As microbiome science progresses a
61 greater understanding of the capabilities of the gut microbiome, and not just its composition,
62 is becoming increasingly the focus.

63 Increased presence of certain *Lachnospiraceae* in the human gut is associated with
64 weight gain and antibiotic use [11–13]. *Clostridium* (a member of the *Lachnospiraceae* family)
65 is a key genus within the gut microbiome known to modulate host immune and metabolic
66 processes [14–16]. The current taxonomic classification of the genus *Clostridium* comprises
67 approximately 150 metabolically diverse species of anaerobes. The genus is almost
68 ubiquitous in anoxic habitats where organic compounds are present, such as soils, aquatic
69 sediments, and the intestinal tracts of animals and humans [17]. Genome sizes differ
70 significantly among *Clostridia* with the larger genomes of certain *Lachnospiraceae* species
71 such as *Clostridium clostridioforme* (more recently reclassified as *Enterocloster*
72 *clostridioformis*) and *Clostridium bolteae* hypothesized to contain genomic features that
73 underlie their ability to colonize the disrupted intestinal microbiome, likely by means of
74 increased metabolic capabilities [11, 12, 18]. *C. bolteae* populations are known to significantly
75 increase in number post-antibiotic treatment in the human gut, and this increase can persist

76 for 180 days post-treatment [11, 12]. *Lachnospiraceae* species such as *C. clostridioforme* are
77 also significantly increased in the gut microbiome of patients with type 2 diabetes mellitus and
78 autism spectrum disorders, and are discriminatory of the low gene content in the intestine
79 associated with obesity, while increases in *C. symbiosum* numbers have been associated with
80 colorectal cancer [13, 19–22]. Given their links to metabolic disease, dietary changes, cancer
81 and antibiotic use, the increased presence of these strains of *Lachnospiraceae* in the intestine
82 under certain conditions has been taken to be indicative of a Western lifestyle.

83 Alteration of the human gut microbiome occurs through multiple mechanisms including
84 dietary selection, as evidenced by the changing gut microbiome in infants as they progress to
85 adulthood, and also through insults such as environmental changes, various disease states,
86 and medical interventions such as the use of antibiotics [11, 12, 23–25]. These can result in
87 distinctive shifts in human gut microbiota profiles with specific families or species of bacteria
88 increasing or decreasing in number in response to change. Why some microbes succeed and
89 proliferate over others under such circumstances is incompletely understood, but hypotheses
90 include increased antibiotic resistance and metabolic capabilities in those strains that
91 successfully respond to change [11, 12, 23]. Here we characterize in detail recently-isolated
92 strains of *C. clostridioforme* and *C. symbiosum*, two species that proliferate in response to
93 perturbations of the gut microbiota as well as producing novel metabolites of significance for
94 mammalian health [9]. We undertook comparative genomic and phylogenetic analysis of these
95 poorly characterized species. The *C. clostridioforme* and *C. symbiosum* strains isolated and
96 sequenced here have significantly larger genomes with a significantly increased number and
97 diversity of mobile genetic elements (MGEs) in comparison with closely related strains. Our
98 findings indicate that the *C. clostridioforme* strains isolated here have an unusual ability to
99 harbour, and likely also acquire, MGEs with their increased genome size largely attributable
100 to these elements.

101

102

103

104 **Materials and methods**

105 **Bacterial strains and growth conditions.**

106 Bacterial strains were isolated by removal of the whole intestine from mice and culturing the
107 gut contents on fastidious anaerobe broth (FAB) agar (Neogen, UK) at 37°C under anaerobic
108 conditions. The sequenced isolates were isolated from a Fragile X syndrome mouse (*Fmr1*^{-/y})
109 colony (*Fmr1* KO mouse) [26]. Selected colonies were grown on solid FAB media and 16S
110 rDNA PCR was carried out as previously described [9] enabling the establishment of putative
111 identities based on 16S rDNA analysis. In preparation for sequencing all strains were grown
112 in liquid cultures prepared by inoculating a single isolated colony into FAB (Neogen, UK) and
113 growing at 37°C without shaking in an anaerobic cabinet.

114

115 **Genome sequencing**

116 Genomes of the four strains, putatively identified by 16S rDNA sequencing as *Clostridium*
117 *symbiosum* (strains LM19B and LM19R) and *Clostridium clostridioforme* (strains LM41A and
118 LM42D), were obtained using two sequencing technologies. First, bacterial lawns were
119 generated from single colonies. Genomic DNA was extracted using Purelink Genomic DNA
120 kit (Invitrogen K182001). Widened pipette tips were used to maintain higher molecular weight
121 DNA. Additionally, the protocol from Invitrogen was altered as to not include any vortexing but
122 instead shaking to prevent excess DNA shearing. The final elution step was carried out in
123 distilled water rather than the kit elution buffer to allow better downstream processing and the
124 samples sent to MicrobesNG (Birmingham University, UK) for Illumina and MinION hybrid
125 sequencing. The draft genomes have been deposited at GenBank in BioProject
126 PRJNA936716; and under BioSample numbers; LM19B; SAMN33749590, LM19R;
127 SAMN33749591, LM41; SAMN33749588 and LM42; SAMN33749589.

128

129 **Genomic analysis**

130 Genome analysis was conducted using CLC genomics workbench (v.7.0.1) and comparative
131 genomic analysis performed through OrthoFinder v2.5.2, Prodigal v2.6.3 and Roary v3.12.0
132 [22–24]. Open reading frames were found using Glimmer3.02 [27]. Pairwise average
133 nucleotide identities were calculated for the four sequenced isolates *Clostridium symbiosum*
134 LM19B, *Clostridium symbiosum* LM19R, *Clostridium clostridioforme* LM41A and *Clostridium*
135 *clostridioforme* LM42D, alongside 162 *Lachnoclostridium* (NCBI:txid1506553) genomes
136 downloaded from NCBI on 13th December 2019. Genomes were downloaded with, and ANIm
137 calculated using, pyani v0.3.0a1 [27]. AntiSMASH (v4.1.0) was used to analyse secondary
138 metabolite production [25]. Phage detection in the bacterial strains was undertaken using
139 Phaster [26]. Transposons were detected with Tn Central [28] and integrative elements were
140 detected using ICEfinder v1.0 [29]. Plasmids in *C. clostridioforme* strains LM41 and LM42
141 were annotated using RAST and ORF identities were then manually curated using BLAST
142 v2.12.0 [30, 31].

143

144 **Results**

145 **Increased genome size in *C. clostridioforme* strains LM41 and LM42**

146 The *C. clostridioforme* strains isolated and sequenced here, LM41 and LM42, at 7.78 Mb had
147 larger genomes than those of all other *C. clostridioforme* and *Clostridium* XIVa strains obtained
148 from NCBI (range of genome size 5.4 – 6.7 Mb) (Table 1). The closest strain in size was *C.*
149 *clostridioforme* YL32 which, at 7.2 Mb, was only 0.6 Mb smaller and also grouped more closely
150 phylogenetically with LM41 and LM42 (Fig. 1). Both *C. symbiosum* strains, LM19B (5.29 Mb)
151 and LM19R (5.29 Mb), were comparable in size to that of a *C. symbiosum* LT0011 reference
152 isolate. *C. clostridioforme* LM41 and LM42 had the lowest GC content of all sequenced *C.*
153 *clostridioforme* strains while *C. symbiosum* LM19B and LM19R had comparable GC content
154 to other *C. symbiosum* strains (Table 1).

155 Whole-genome average nucleotide identity (ANIm) analysis was conducted for the 4
156 isolated strains and 162 *Lachnoclostridium* genomes obtained from GenBank, and ten
157 additional isolates using pyani v0.3.0a1 [27]. The resulting plot indicated more than 20 groups

158 of sequenced isolates that, in pairwise alignments, mutually share at least 50% of their
159 genomic material with each other but share only a small proportion (0-10%) of their sequenced
160 genome with any other group (Fig. 2). In other families, these groupings are seen to coincide
161 with recognised genus-level taxonomic divisions, implying that the existing *Lachnoclostridium*
162 genus classification may benefit from genome-informed taxonomy revision.

163 The largest such grouping (group 1) contains 48 genome sequences, including
164 sequenced isolates *C. clostridioforme* LM41, LM42, 90A7, CM201 and YL32 and *C. bolteae*
165 BAA613, and all NCBI-downloaded isolates assigned as *C. bolteae* or *C. clostridioforme*. The
166 next-largest grouping (group 2) contains 17 genome sequences, including *C. symbiosum*
167 isolates LM19B, LM19R, LT0011, and C14940, and all NCBI-downloaded isolates assigned
168 as *C. symbiosum*. We refer to these as the (1) *C. bolteae/C. clostridioforme* and (2) *C.*
169 *symbiosum* groups respectively but note that this genomic evidence supports nomenclature
170 reassignment of these groups at genus-level (Fig. 2).

171 All genomes in the *C. symbiosum* grouping share at least 77% of their total genomic
172 sequence in homologous alignment with other members of the grouping. The *C. symbiosum*
173 LM19B and LM19R genomes share nearly 100% of their genomes with each other in this way,
174 but only 77-83% with the other *C. symbiosum* genomes, indicating that approximately 20% of
175 the LM19B and LM19R genomes are unique to those strains, among the sequenced isolates.

176 The *C. bolteae/C. clostridioforme* grouping is divisible into four major subgroups. The
177 collection of *C. bolteae* isolates each share at least 73% of their genome in homologous
178 alignment, but no more than 57% of their genome with the other members of the larger
179 grouping. Similarly, the *C. clostridioforme* isolates share at least 62% (and usually at least
180 75% of their genomes in homologous alignment with other members of the *C. clostridioforme*
181 group), but (mostly) no more than 66% with any other member of the larger grouping. The
182 remaining groups are complex, and include the *C. clostridioforme* grouping of isolates YL32,
183 LM41 and LM42. The *C. clostridioforme* set share at least 67% of their genomes with these
184 three isolates; however, YL32, LM41 and LM42 share no more than 60% of their genomes
185 with any *C. clostridioforme* genome. This asymmetry indicates that a considerable amount of

186 material that is not homologous to the other *Clostridia* in this study has been incorporated into
187 the genomes of these three isolates. Specifically, the alignments of LM41 and LM42 share 7.6
188 Mbp of genome sequence with each other, 4.7 Mbp with YL32, but no more than 4.5 Mbp with
189 other *C. clostridioforme*. Likewise, YL32 (genome size: 7.2 Mbp) alignments share no more
190 than 4.3 Mbp with any other *C. clostridioforme*.

191 ANIm analysis indicates that *C. symbiosum* (minimum 99% identity), *C. bolteae*
192 (minimum 97% identity) and *C. clostridioforme* (minimum 98% identity) constitute distinct
193 species groups and belong to the same genus (Fig. 2). Some isolates appear to have been
194 assigned to an incorrect species (e.g., *C. clostridioforme* AM07-19 and 90A7, which we identify
195 as *C. bolteae*), and two isolates (*C. bolteae* W0P9.022 and *C. clostridioforme* AGR2 157)
196 appear to be the single examples of distinct novel species; W0P9.022 shares no more than
197 7.5% of homologous genome sequence with any of the other isolates in the figure and so
198 should be considered to belong to a distinct genus.

199 Despite the additional genomic material noted above, homologous alignment with the
200 other members of their groups unambiguously places isolates LM41 and LM42 as *C.*
201 *clostridioforme* and LM19B and LM19R as *C. symbiosum*, taxonomically. Reannotation of the
202 55 *C. bolteae*, *C. clostridioforme*, and *C. symbiosum* genomes identified above (excluding
203 W0P9.022) using Prokka, followed by pangenome analyses with Roary, suggests core
204 genome sizes consistent with other bacterial species for *C. clostridioforme* (1898 genes), *C.*
205 *bolteae* (3085 genes) and *C. symbiosum* (2936 genes) (Figure 3, Table 2 and Supplementary
206 Figures 1-3). In *C. symbiosum* 47% of total genes were determined to be “cloud” genes (5125
207 of 10887 genes) while in *C. bolteae* this was 50% (7698 of 15420 genes). In *C. clostridioforme*
208 however there was a significant increase in size of the accessory genome 55% of genes, of
209 the total of 25402, identified as cloud genes.

210

211 **Increased phage carriage in *C. clostridioforme* LM41 and LM42**

212 Given the relative increase in size of the accessory genome of *C. clostridioforme*
213 isolates LM41 and LM42 in comparison to other *C. clostridioforme* strains, we sought to

214 determine whether acquisition of new genetic material through mobile genetic elements
215 (MGEs) could account for at least some of the increase in genome size. Initially, using the
216 phage search tool Phaster [32], a significantly increased number of putative prophages were
217 predicted in LM41 and LM42 in comparison to other *C. clostridioforme* strains (Table 3). These
218 putative prophages comprised over 12% of the total genome in both these strains, more than
219 double the genetic material ascribed to predicted prophages in any other *C. clostridioforme*
220 strain, except for the most closely related strain YL32 in which 8.6% of its genome was
221 determined to be of likely prophage origin. Predicted prophage material made up between 1.9
222 and 5.5 % of all other *C. clostridioforme* strain genomes, with all these strains also having
223 significantly smaller genomes than *C. clostridioforme* LM41, LM42 and YL32 (Table 3). While
224 many predicted prophages were common to both *C. clostridioforme* LM41 and LM42, a
225 number of these differed between the strains (Table S1).

226 For *C. symbiosum* strains LM19B and LM19R a similar evolution towards increased
227 prophage tolerance was noted. These strains, with significantly smaller genomes than *C.*
228 *clostridioforme* (5.29 Mb versus 7.78 Mb respectively), were identified as each having 8
229 prophages, comprising just under 5% of the total genome (Table 3). This was a significant
230 increase in predicted phage number compared to the other *C. symbiosum* strains, which all
231 have fewer prophages, except for WAL-14163 which had 12 predicted prophages that make
232 up over 7% of its total genetic material. *C. bolteae* isolates had a range of phage numbers
233 comprising anywhere from 0.1 to 7 % of their total genome across the 18 sequenced strains.
234 However, the majority had few, if any, predicted intact prophages, and none had greater than
235 4% of their genome annotated as being phage derived. While 29 and 28 prophages were
236 predicted in *C. clostridioforme* LM41 and LM42 respectively, these are likely not all functional
237 and will need to be investigated further.

238 With the large number of predicted prophages in *C. clostridioforme* strains LM41 and
239 LM42, and the comparable genome sizes between the strains (7.78 Mb for each), it was
240 hypothesized that these strains derive from a recent common ancestor. However further
241 examination of the prophage content of each strain indicated that, of the prophages present

242 in each, only 23 were common to both *C. clostridioforme* LM41 and LM42 with each having at
243 least 5 unique predicted prophage elements (Supplementary Table 1). Additionally, many
244 prophages were distributed and orientated differently in each isolate. In the case of *C.*
245 *symbiosum* strains LM19B and LM19R no phage was found that was predicted to be common
246 to both strains (data not shown).

247

248 **Increased presence of MGEs other than phage in *C. clostridioforme* LM41 and LM42**

249 *C. clostridioforme* LM41 and LM42 both carried an identical large plasmid of 192,394
250 bp in size (pCclLM41_1 and pCclLM42_1 respectively). The plasmid had a significantly lower
251 GC content than either genome, at 44.6% GC (versus 47.8% for each genome). It was highly
252 stable, and despite attempts to cure *C. clostridioforme* LM41 of the plasmid over 12 weeks
253 through repeated subculturing in nutrient rich media it was retained. No single nucleotide
254 polymorphisms (SNPs) appeared over this time (data not shown). The plasmid contains a
255 number of intriguing predicted ORFs, in the context of intestinal colonisation. The first
256 predicted protein was very large, 3824 amino acids in length, and bears significant homology
257 to the approximately 500 amino acid SpaA isopeptide forming pilin-like protein from
258 *Corynebacterium diphtheriae* [33]. However, rather than encoding a pilin monomer, the SpaA
259 motif was identified as repeating 15 times within this protein. SpaA-derived pilins play an
260 important role in *C. diphtheriae* virulence, enabling attachment to specific tissues, suggesting
261 that this large protein possibly encodes a protein with a similar contribution to adhesion in *C.*
262 *clostridioforme* [33]. Additionally, a BGC containing a large non-ribosomal peptide synthetase
263 (NRPS) of 2759 amino acids was identified in the plasmid next to a Sec system translocase.
264 This NRPS is predicted by antiSmash to encode for an enniatin-like antimicrobial.

265 The larger genome size and accessory genomes of *C. clostridioforme* LM41 and LM42,
266 in comparison to other strains of *C. clostridioforme*, motivated detailed examination of these
267 genomes for the presence of MGEs other than prophages and plasmids, that may contribute
268 to the genome size difference. We found evidence for the abundant presence of multiple types
269 of MGEs. Using the ICEfinder tool to search the *C. clostridioforme* LM41 genome we identified

270 seven putative integrative and conjugative elements (ICE), each with an associated type 4
271 secretion system (T4SS), and five putative integrative and mobilizable elements (IME),
272 alongside what is termed an *Agrobacterium tumefaciens* integrative and conjugative element
273 (AICE) (Table 4) [29]. A more diverse array of ICEs and IMEs was identified in *C.*
274 *clostridioforme* LM42: 17 in total including eight putative ICEs with their own T4SS and nine
275 IMEs. These elements differed significantly in their size and distribution between LM41 and
276 LM42. *C. symbiosum* LM19B contained two putative IMEs and a single ICE while *C.*
277 *symbiosum* LM19R had three putative IMEs and two putative ICEs, but there was low
278 sequence identity between the regions from both *C. symbiosum* LM19B and LM19R, and a
279 significant size discrepancy between them (Table 4). IS66 transposases were predicted in a
280 number of putative phage regions identified by Phaster in the genomes of *C. clostridioforme*
281 LM41 and LM42, potentially leading to their misidentification as phage elements [32]. Further
282 examination of the genome of *C. clostridioforme* LM41 indicated the presence of 27 identical
283 copies of the IS66 transposase (each at 1623 bp and 100% nucleotide identity), alongside two
284 further copies that were either partial or not identical. Additionally, a further two identical copies
285 of IS66 were identified on the plasmid alongside a further partial copy. Each IS66 had what
286 has been deemed a classic organisation with the *tnpC* transposase gene accompanied by
287 accessory proteins [34]. The presence of multiple copies of the IS66 in the genome and on
288 the associated plasmid, with identical nucleotide sequence, is suggestive of high levels of
289 mobility within the genome. Further transposons were identified using the Tn Central search
290 tool [29]. In the *C. clostridioforme* LM41 chromosome, 43 transposon elements were identified
291 from a variety of transposon element families with five of these being described as insertion
292 sequences and one being described as an integron. These varied in size from small insertion
293 sequences of just over 1 Kb to larger transposon elements of close to 28 Kb, and in total were
294 predicted to comprise 497 Kb (6.3%) of the LM41 genome. Again 43 transposon elements
295 were identified in *C. clostridioforme* LM42, while 23 were identified in each of *C. symbiosum*
296 LM19B and LM19R. In contrast to the differences in phage presence no difference in

297 transposon carriage, or identity, was noted between the *C. clostridioforme* LM41 and LM42 or
298 *C. symbiosum* strains LM19B and LM19R.

299 Intriguingly, 23 copies, alongside two partial copies, of a gene homologous to the *ltrA*
300 gene found in group II introns were identified in the LM41 genome. Group II introns are often
301 termed 'selfish' due to their apparent lack of benefit to the host bacterium but they may alter
302 splicing, thus increasing genetic diversity through alteration of the bacterial transcriptome [35,
303 36]. The *ltrA* gene encodes a protein with multiple functions that enable the excision, mobility
304 and insertion of this intron in a genome. These functions were all predicted to be encoded in
305 the 23 complete *ltrA* genes identified in LM41. While *ltrA* gene presence alone is insufficient
306 to definitively confirm the presence of a functional group II intron, without identification of the
307 surrounding RNA sequence essential to splicing, it indicates the potential presence of
308 significant number of these introns and, to our knowledge, far more than have to date to been
309 described in any other bacterial genome.

310

311 ***Secondary metabolite production in Clostridium XIVa species***

312 To understand what potential competitive advantage may be conferred by increased
313 genome size, antiSmash was used to determine the presence of predicted secondary
314 metabolite encoding biosynthetic gene clusters (BGCs) in each genome [37]. *C. symbiosum*
315 LM19B and LM19R putatively encode for a single ranthipeptide through an identified BGC,
316 and a highly similar cluster was also found in other strains such as *C. symbiosum*
317 WAL14163 (Table 5). In contrast *C. clostridioforme* LM41 and LM42 are predicted to encode
318 a much larger number and variety of BGCs. In total ten BGCs were predicted in the genome
319 of each strain and again *C. clostridioforme* YL32 was the only other sequenced *C.*
320 *clostridioforme* containing a comparable number of predicted BGCs, with 13. Twenty other
321 *C. clostridioforme* strains studied had either one or two putative BGCs, while two other
322 strains had three and five predicted BGCs respectively. In *C. clostridioforme* LM41 and
323 LM42 BGCs for NRPS-like (x2), transAT-PKS, lanthipeptide-class-ii, cyclic-lactone-
324 autoinducer (x4), NRPS (butyrolactone related) and ranthipeptide were predicted. A number

325 of these BGCs were unique with little sequence identity to known BGCs. BGCs predicted in
326 *C. clostridioforme* YL32 were similar to those in LM41 and LM42 with the major difference
327 being in quantity of each encoded on the YL32 genome (e.g. eight cyclic-lactone
328 autoinducers in YL32 versus four in each of LM41 and LM42). The pCclLM41_1 and
329 pCclLM42_1 plasmids also encoded a single BGC for an NRPS.

330

331 **Discussion**

332 *Lachnospiraceae* are intrinsically linked to Western disease, their presence in the
333 human gut being associated with obesity and antibiotic use [11–13]. They possess a large
334 number of antibiotic resistance genes that may explain their ability to respond positively to
335 antibiotic treatment by proliferating in the months following treatment [11, 12, 38].
336 *Lachnospiraceae* adapt well to dysbiosis and are associated with conditions with known
337 microbiome perturbances such as type 2 diabetes and autism spectrum disorders, as well as
338 significantly changing in abundance over the first two years of life [20, 21, 23, 39]. Their
339 increased presence upon dysbiosis in the human intestine has previously been linked to their
340 often-large genome size, with their genomes being significantly larger than other commensal
341 bacteria and potentially conferring increased metabolic flexibility [23]. However, despite their
342 abundance in the mammalian gut microbiome and their association with specific conditions,
343 *Lachnospiraceae* remain relatively poorly understood. Here, using recently isolated
344 *Clostridium symbiosum* and *Clostridium clostridioforme* strains from the murine gut
345 microbiome, we demonstrate how these strains have exceptionally large genomes even in
346 comparison to other closely related strains. An unusual ability to acquire and maintain a
347 significant number of MGEs seems, at least in part, to underlie this increased genome size.

348 Through phylogenetic relatedness and comparison to reference genomes of *Clostridia*
349 sp. we were able to assign isolates LM19B and LM19R as *C. symbiosum* and isolates LM41
350 and LM42 as *C. clostridioforme*. Although the genome sizes of LM19B (5.29 Mbp) and LM19R
351 (5.29 Mbp) were comparable to that of *C. symbiosum* reference isolate LT0011 (5 Mbp), those
352 of isolates LM41 (7.79 Mbp) and LM42 (7.79 Mbp) are significantly larger than other

353 sequenced *C. clostridioforme* strains with the majority of strains being between 5.5-6.5 Mb in
354 length. LM41 and LM42 were phylogenetically most closely related to strain YL32, a strain of
355 similarly increased genome size (7.2 Mbp), and these genomes were found to be highly similar
356 by ANI. *C. clostridioforme* was previously reclassified into three species, *C. hathewayi*, *C.*
357 *bolteae* and *C. clostridioforme* [38, 40, 41], and it has recently been suggested that these
358 phylogenetically similar organisms should be reclassified further [42].

359 In conjunction with their large size *C. clostridioforme* genomes show clear evidence of
360 genome plasticity with a smaller core genome (1898 genes) in comparison to both *C.*
361 *symbiosum* (2936 genes) and *C. bolteae* (3085 genes), both of which have shorter genomes
362 but larger core gene sets. We investigated the large accessory genome in *C. clostridioforme*
363 strains LM41 and LM42 and determined it to be in part due to a significant increase in the
364 presence of prophages in each genome with greater than 10% of each genome predicted to
365 be phage derived. Present dogma dictates that evolutionary pressures would result in loss
366 over time of such prophages with their presence negatively impacting competitiveness, due to
367 the burden of replicating such a large collection of prophages. Therefore the presence of such
368 a high number of prophages, particularly in direct contrast to closely related *C. clostridioforme*
369 strains, is intriguing and certainly worthy of further study. There was scant evidence to suggest
370 these prophages were providing any selective advantage to LM41 or LM42. No antibiotic
371 resistance genes were found in any of the prophages and while there was a predicted increase
372 in secondary metabolite production capability as per antiSmash analysis, none of these novel
373 BGCs were associated with prophages [37]. Therefore the role of these prophages in the
374 context of bacterial survival in the murine gut is unclear. During times of inflammation or
375 perturbation of the microbiome when phages are plentiful in the gut, the possession of a large
376 number of phages such as found in LM41 and LM42 may provide some protection against
377 further phage infection through competitive exclusion, mediated by phages in the genome [43].
378 Interestingly, relatively high numbers of prophages were also predicted in *C. symbiosum*
379 LM19B and LM19R. Whether selective pressures in the murine gut are affecting prophage
380 infection of, and retention in, *Lachnospiraceae* is worthy of further investigation as it may

381 have ramifications for other environmental niches where such microbiome disturbances are
382 established.

383 The presence of an identical and highly stable plasmid in both the LM41 and LM42
384 strains was interesting due to the large size of the plasmid, the difference in GC content in
385 comparison to the genome, and an extremely large ORF carried on the plasmid. The
386 difference in GC content indicates the plasmid likely has an origin other than related
387 *Clostridium* XIVa strains as the GC content is substantially lower than all *Clostridium* XIVa
388 strains sequenced to date. Also, there is no evidence that the sequenced strain most closely
389 related phylogenetically to LM41 and LM42, YL32, carries such a plasmid. We consider that
390 acquisition *in vivo* is the most plausible reason for its carriage and, alongside the multiple other
391 MGEs found in LM41 and LM42, underlines the promiscuity of these *C. clostridioforme* strains
392 in terms of DNA acquisition.

393 Analysis of the LM41 genome in detail highlighted the presence of 29 identical copies
394 of the IS66 transposase, along with 4 truncated copies and numerous other transposons. The
395 fact that the IS66 transposase was 100% identical in each case across its total nucleotide
396 sequence was intriguing and perhaps indicated either recent multiple acquisition events or,
397 more likely, recent reproduction of the transposase genes and their insertion at multiple sites.
398 The IS66 transposons were judged to be classic in that each encoded accessory ORFs such
399 as TnpB alongside the TnpC transposase [34]. Given these findings, which indicated that
400 LM41 was highly promiscuous in uptake of MGEs, we searched for evidence of integrative
401 conjugative elements (ICE) and integrative and mobilizable elements (IME) as well as other
402 MGEs such as group II introns. While ICEs and IMEs were detected, an unusually high number
403 of copies of the group II intron-associated *ltrA* gene were detected. Although its presence is
404 not definitive evidence of a functioning intron without identification of surrounding regions
405 essential for splicing, we identified 23 complete *ltrA* genes. Given that the putative role of these
406 MGEs is to alter the bacterial transcriptome through alternative splicing of bacterial genes, it
407 is possible that the unprecedented number of *ltrA* genes found in these *C. clostridioforme*
408 strains is indicative of further genome plasticity [35]. This alternative splicing could confer on

409 these strains additional capabilities beyond those already afforded by the significantly
410 increased genome size.

411 Given the increased gene flow seen as a result of HGT in *C. clostridioforme* strains
412 LM41, LM42 and YL32 it raises the question of whether defence systems to combat phage
413 and MGEs are present in lower numbers or are less efficient in these strains. While a lack of
414 such systems, be they restriction modification, CRISPR-Cas or similar, would expose the
415 strains to increased risk due to increased virulent phage infection or propagation, it would
416 explain the increased presence of phage and MGEs in these strains, their widespread
417 distribution in the genomes and the significantly increased size comparable to other *C.*
418 *clostridioforme* genomes.

419 In conclusion, we have characterised the genome sequences of newly isolated and
420 highly unusual strains of *Lachnospiraceae*. Our study has revealed that while the *C.*
421 *symbiosum* strains identified have similar genome sequences to those of the reference strains,
422 the genomes of the newly sequenced *C. clostridioforme* strains are substantially larger than
423 those previously sequenced, with the single exception of *C. clostridioforme* YL32. YL32's
424 genome is not as large as the two *C. clostridioforme* strains identified here but shows similar
425 increases in secondary metabolite production capability and prophage presence. Additionally,
426 *C. clostridioforme* YL32 and the strains isolated here form a monophyletic clade with unusually
427 long branch length in the *C. clostridioforme* phylogenetic tree, consistent with the proposition
428 that increased MGE presence may be a significant evolutionary driver. This work highlights
429 both the potential capabilities and extraordinary complexity within the gut microbiome and
430 emphasizes the significant gaps in our knowledge as regards specific species, the role of MGEs
431 in shaping species evolution in the intestine and the untapped secondary metabolite
432 capabilities of many yet to be identified strains.

433

434

435

436

437 **References**

- 438 1. Nemet I, Saha PP, Gupta N, Zhu W, Romano KA, Skye SM, et al. A Cardiovascular
439 Disease-Linked Gut Microbial Metabolite Acts via Adrenergic Receptors. *Cell*. 2020;180:862-
440 877.e22.
- 441 2. Quinn RA, Melnik A V., Vrbanac A, Fu T, Patras KA, Christy MP, et al. Global chemical
442 effects of the microbiome include new bile-acid conjugations. *Nature*. 2020;579:1–19.
443 doi:10.1038/s41586-020-2047-9.
- 444 3. Foster JA, McVey Neufeld KA. Gut-brain axis: How the microbiome influences anxiety and
445 depression. *Trends in Neurosciences*. 2013.
- 446 4. Carding S, Verbeke K, Vipond DT, Corfe BM, Owen LJ. Dysbiosis of the gut microbiota in
447 disease. *Microb Ecol Heal Dis*. 2015.
- 448 5. Dalile B, Van Oudenhove L, Vervliet B, Verbeke K. The role of short-chain fatty acids in
449 microbiota–gut–brain communication. *Nature Reviews Gastroenterology and Hepatology*.
450 2019.
- 451 6. Fröhlich EE, Farzi A, Mayerhofer R, Reichmann F, Jačan A, Wagner B, et al. Cognitive
452 Impairment by Antibiotic-Induced Gut Dysbiosis: Analysis of Gut Microbiota-Brain
453 Communication. *Brain Behav Immun*. 2016.
- 454 7. Yano JM, Yu K, Donaldson GP, Shastri GG, Ann P, Ma L, et al. Indigenous bacteria from
455 the gut microbiota regulate host serotonin biosynthesis. *Cell*. 2015;161:264–76.
456 doi:10.1016/j.cell.2015.02.047.
- 457 8. Patterson E, Ryan PM, Wiley N, Carafa I, Sherwin E, Moloney G, et al. Gamma-
458 aminobutyric acid-producing lactobacilli positively affect metabolism and depressive-like
459 behaviour in a mouse model of metabolic syndrome. *Sci Rep*. 2019;9:16323.
460 doi:10.1038/s41598-019-51781-x.
- 461 9. Hulme H, Meikle LM, Strittmatter N, van der Hooft JJJ, Swales J, Bragg RA, et al.
462 Microbiome-derived carnitine mimics as previously unknown mediators of gut-brain axis
463 communication. *Sci Adv*. 2020;6:eaax6328.
- 464 10. Hulme H, Meikle LM, Strittmatter N, Swales J, Hamm G, Brown SL, et al. Mapping the

465 Influence of the Gut Microbiota on Small Molecules across the Microbiome Gut Brain Axis. *J*
466 *Am Soc Mass Spectrom.* 2022;33:649–59. doi:10.1021/JASMS.1C00298.

467 11. Raymond F, Ouameur AA, Déraspe M, Iqbal N, Gingras H, Dridi B, et al. The initial state
468 of the human gut microbiome determines its reshaping by antibiotics. *ISME J.* 2016;10:707–
469 20.

470 12. Palleja A, Mikkelsen KH, Forslund SK, Kashani A, Allin KH, Nielsen T, et al. Recovery of
471 gut microbiota of healthy adults following antibiotic exposure. *Nat Microbiol.* 2018;3:1255–
472 65. doi:10.1038/s41564-018-0257-9.

473 13. Le Chatelier E, Nielsen T, Qin J, Prifti E, Hildebrand F, Falony G, et al. Richness of
474 human gut microbiome correlates with metabolic markers. *Nature.* 2013;500:541–6.
475 doi:10.1038/nature12506.

476 14. Pryde SE, Duncan SH, Hold GL, Stewart CS, Flint HJ. The microbiology of butyrate
477 formation in the human colon. *FEMS Microbiol Lett.* 2002;217:133–9. doi:10.1111/j.1574-
478 6968.2002.tb11467.x.

479 15. Jafari N V., Kuehne SA, Bryant CE, Elawad M, Wren BW, Minton NP, et al. *Clostridium*
480 *difficile* Modulates Host Innate Immunity via Toxin-Independent and Dependent
481 Mechanism(s). *PLoS One.* 2013;8:e69846. doi:10.1371/JOURNAL.PONE.0069846.

482 16. Chen H, Ma X, Liu Y, Ma L, Chen Z, Lin X, et al. Gut Microbiota Interventions With
483 *Clostridium butyricum* and Norfloxacin Modulate Immune Response in Experimental
484 Autoimmune Encephalomyelitis Mice. *Front Immunol.* 2019;10:1662.

485 17. Wells CL, Wilkins TD. Clostridia: Sporeforming Anaerobic Bacilli. *Med Microbiol.* 1996.
486 <https://www.ncbi.nlm.nih.gov/books/NBK8219/>. Accessed 4 May 2022.

487 18. Lozupone C, Faust K, Raes J, Faith JJ, Frank DN, Zaneveld J, et al. Identifying genomic
488 and metabolic features that can underlie early successional and opportunistic lifestyles of
489 human gut symbionts. *Genome Res.* 2012;22:1974–84. doi:10.1101/gr.138198.112.

490 19. Karlsson FH, Tremaroli V, Nookaew I, Bergström G, Behre CJ, Fagerberg B, et al. Gut
491 metagenome in European women with normal, impaired and diabetic glucose control. 2013.
492 doi:10.1038/nature12198.

493 20. Qin J, Li Y, Cai Z, Li S, Zhu J, Zhang F, et al. A metagenome-wide association study of
494 gut microbiota in type 2 diabetes. *Nature*. 2012;490:55–60. doi:10.1038/nature11450.

495 21. Finegold SM, Molitoris D, Song Y, Liu C, Vaisanen M, Bolte E, et al. Gastrointestinal
496 Microflora Studies in Late-Onset Autism. *Clin Infect Dis*. 2002.

497 22. Xie YH, Gao QY, Cai GX, Sun XM, Zou TH, Chen HM, et al. Fecal Clostridium
498 symbiosum for Noninvasive Detection of Early and Advanced Colorectal Cancer: Test and
499 Validation Studies. *EBioMedicine*. 2017;25:32–40.

500 23. Lozupone C, Faust K, Raes J, Faith JJ, Frank DN, Zaneveld J, et al. Identifying genomic
501 and metabolic features that can underlie early successional and opportunistic lifestyles of
502 human gut symbionts. *Genome Res*. 2012.

503 24. Yatsunenko T, Rey FE, Manary MJ, Trehan I, Dominguez-Bello MG, Contreras M, et al. Human gut microbiome viewed across age and geography. *Nature*. 2012;486:222–7.

504 25. Stanislawski MA, Dabelea D, Wagner BD, Iszatt N, Dahl C, Sontag MK, et al. Gut
505 Microbiota in the First 2 Years of Life and the Association with Body Mass Index at Age 12 in
506 a Norwegian Birth Cohort. *MBio*. 2018;9. doi:10.1128/mBio.01751-18.

507 26. Thomson SR, Seo SS, Barnes SA, Louros SR, Muscas M, Dando O, et al. Cell-Type-
508 Specific Translation Profiling Reveals a Novel Strategy for Treating Fragile X Syndrome.
509 *Neuron*. 2017;95:550–563.e5. doi:10.1016/j.neuron.2017.07.013.

510 27. Pritchard L, Glover RH, Humphris S, Elphinstone JG, Toth IK. Genomics and taxonomy
511 in diagnostics for food security: Soft-rotting enterobacterial plant pathogens. *Analytical
512 Methods*. 2016;8:12–24. doi:10.1039/c5ay02550h.

513 28. Ross K, Varani AM, Snesrud E, Huang H, Alvarenga DO, Zhang J, et al. TnCentral: a
514 Prokaryotic Transposable Element Database and Web Portal for Transposon Analysis.
515 *MBio*. 2021;12. doi:10.1128/MBIO.02060-21.

516 29. Liu M, Li X, Xie Y, Bi D, Sun J, Li J, et al. ICEberg 2.0: an updated database of bacterial
517 integrative and conjugative elements. *Nucleic Acids Res*. 2019;47:D660–5.
518 doi:10.1093/NAR/GKY1123.

519 30. Aziz RK, Bartels D, Best A, DeJongh M, Disz T, Edwards RA, et al. The RAST Server:
520

521 rapid annotations using subsystems technology. *BMC Genomics*. 2008;9. doi:10.1186/1471-
522 2164-9-75.

523 31. Altschul SF, Gish W, Miller W, Myers EW, Lipman DJ. Basic local alignment search tool.
524 *J Mol Biol*. 1990.

525 32. Arndt D, Grant JR, Marcu A, Sajed T, Pon A, Liang Y, et al. PHASTER: a better, faster
526 version of the PHAST phage search tool. *Nucleic Acids Res*. 2016;44:W16–21.
527 doi:10.1093/nar/gkw387.

528 33. Hae JK, Paterson NG, Gaspar AH, Hung TT, Baker EN. The *Corynebacterium*
529 diphtheriae shaft pilin SpaA is built of tandem Ig-like modules with stabilizing isopeptide and
530 disulfide bonds. *Proc Natl Acad Sci U S A*. 2009;106:16967–71.
531 doi:10.1073/PNAS.0906826106/SUPPL_FILE/0906826106SI.PDF.

532 34. Gourbeyre E, Siguier P, Chandler M. Route 66: investigations into the organisation and
533 distribution of the IS66 family of prokaryotic insertion sequences. *Res Microbiol*.
534 2010;161:136–43. doi:10.1016/J.RESMIC.2009.11.005.

535 35. LaRoche-Johnston F, Monat C, Coulombe S, Cousineau B. Bacterial group II introns
536 generate genetic diversity by circularization and trans-splicing from a population of intron-
537 invaded mRNAs. *PLoS Genet*. 2018;14. doi:10.1371/JOURNAL.PGEN.1007792.

538 36. Toro N, Martínez-Abarca F, Molina-Sánchez MD, García-Rodríguez FM, Nisa-Martínez
539 R. Contribution of Mobile Group II Introns to *Sinorhizobium meliloti* Genome Evolution. *Front*
540 *Microbiol*. 2018;9 APR. doi:10.3389/FMICB.2018.00627.

541 37. Blin K, Shaw S, Kloosterman AM, Charlop-Powers Z, Van Wezel GP, Medema MH, et al.
542 AntiSMASH 6.0: Improving cluster detection and comparison capabilities. *Nucleic Acids Res*.
543 2021;49:W29–35. doi:10.1093/nar/gkab335.

544 38. Dehoux P, Marvaud JC, Abouelleil A, Earl AM, Lambert T, Dauga C. Comparative
545 genomics of *Clostridium bolteae* and *Clostridium clostridioforme* reveals species-specific
546 genomic properties and numerous putative antibiotic resistance determinants. *BMC*
547 *Genomics*. 2016.

548 39. Karlsson FH, Tremaroli V, Nookaew I, Bergström G, Behre CJ, Fagerberg B, et al. *Gut*

549 metagenome in European women - supply. *Nature*. 2013;498:99–103.
550 doi:10.1038/nature12198.

551 40. Finegold SM, Song Y, Liu C, Hecht DW, Summanen P, Könönen E, et al. *Clostridium*
552 *clostridioforme*: A mixture of three clinically important species. *Eur J Clin Microbiol Infect Dis*.
553 2005;24:319–24. doi:10.1007/s10096-005-1334-6.

554 41. Haas KN, Blanchard JL. Reclassification of the *Clostridium clostridioforme* and
555 *Clostridium sphenoides* clades as *Enterocloster* gen. Nov. and *lacrimispora* gen. nov.,
556 including reclassification of 15 taxa. *Int J Syst Evol Microbiol*. 2020.

557 42. Schaubeck M, Clavel T, Calasan J, Lagkouvardos I, Haange SB, Jehmlich N, et al.
558 Dysbiotic gut microbiota causes transmissible Crohn's disease-like ileitis independent of
559 failure in antimicrobial defence. *Gut*. 2016.

560 43. Rocha EPC, Bikard D. Microbial defenses against mobile genetic elements and viruses:
561 Who defends whom from what? *PLOS Biol*. 2022;20:e3001514.
562 doi:10.1371/JOURNAL.PBIO.3001514.

563

564

565

566

567

568

569

570

571

572

573

574

575

576

577 **Figures**

578 **Figure 1**



579

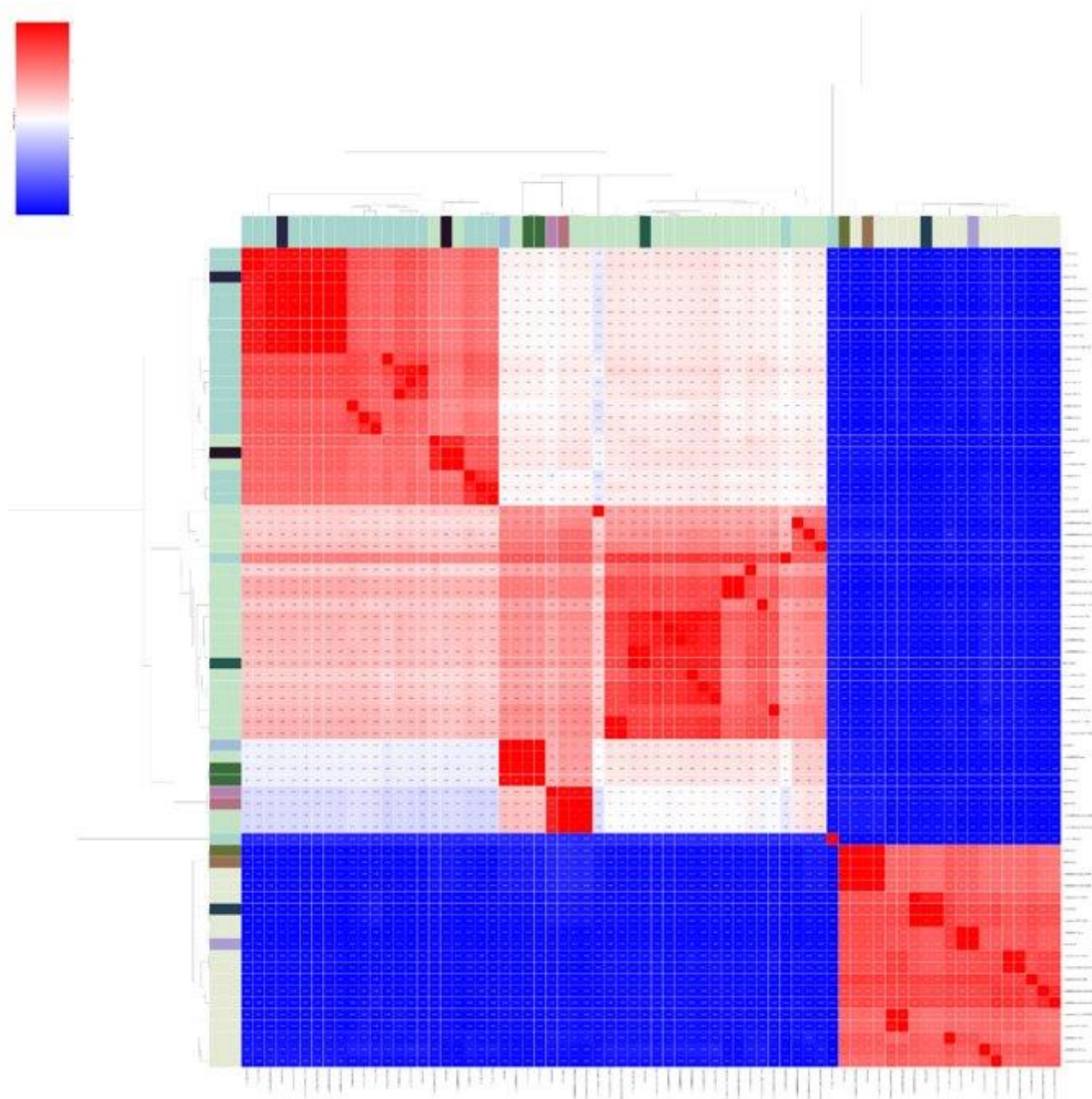
0.06

580 **Figure 1: Identification of phylogenetic lineages of *Clostridia* isolates.** Phylogenetic
581 rooted gene tree of *Clostridium XIVa* cluster created with single copy orthologs (OrthoFinder
582 v2.5.2). New strains identified, LM19B, LM19R, LM41 and LM42 are highlighted with red and
583 can be seen to fall into previously identified *C. symbiosum* and *C. clostridioforme* respectively.

584

585 **Figure 2**

586 **a**



587

588

589

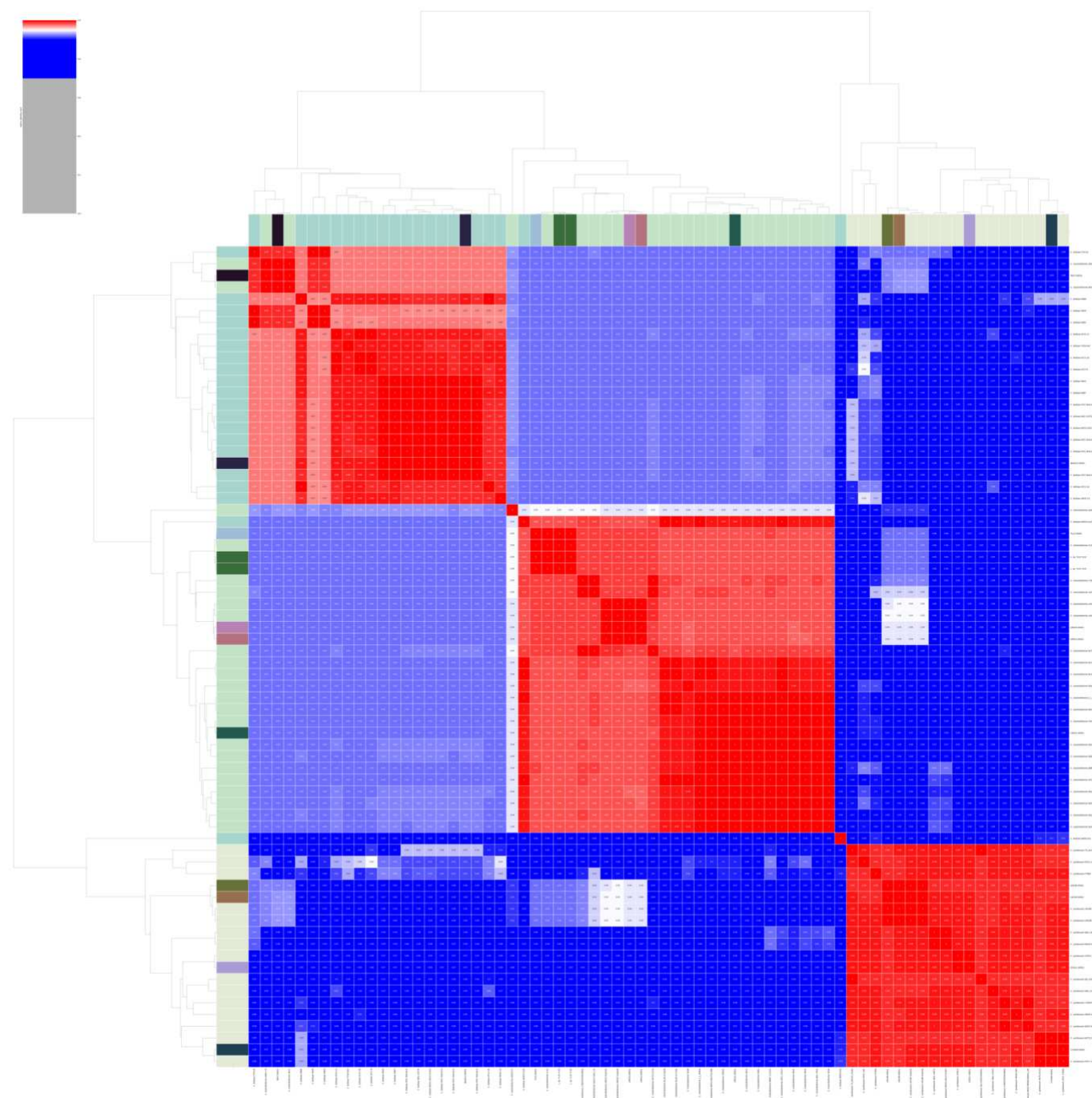
590

591

592

593

b



594

595 **Figure 2: ANIm (Average Nucleotide Identity using MUMmer) comparisons of**
596 ***Clostridium XIVa* cluster genomes obtained using pyani v0.3+.** (a) shows a heat map of
597 genome percent coverage: pairwise comparisons where the alignable fraction of genome is
598 greater than 50% are indicated in red; blue cells indicate that the alignable fraction is less than
599 50% of the genome. *C. bolteae* and *C. clostridioforme* are generally alignable over 50% of
600 their genome sequence but share less than 5% of alignable genome sequence with *C.*

601 *symbiosum*. This indicates that *C. bolteae/C. clostridioforme* are likely to correspond to the
602 same genus, but that they are genomically quite distinct from *C. symbiosum*. **(b)** is a heat map
603 of ANIm percentage identity, where red cells indicate an identity greater than 95% (an
604 approximate threshold for bacterial species boundaries), and blue cells an identity less than
605 95%. The heat map confirms that the sequenced *C. bolteae*, *C. symbiosum*, and *C.*
606 *clostridioforme* isolates support division into the three species groups, but that isolate
607 W0P9.022 may be a member of a distinct species; this conclusion is also supported by the
608 genome coverage data, which suggests that W0P9.022 may also be the sole representative
609 of a distinct genus.

610

611

612

613

614

615

616

617

618

619

620

621

622

623

624

625

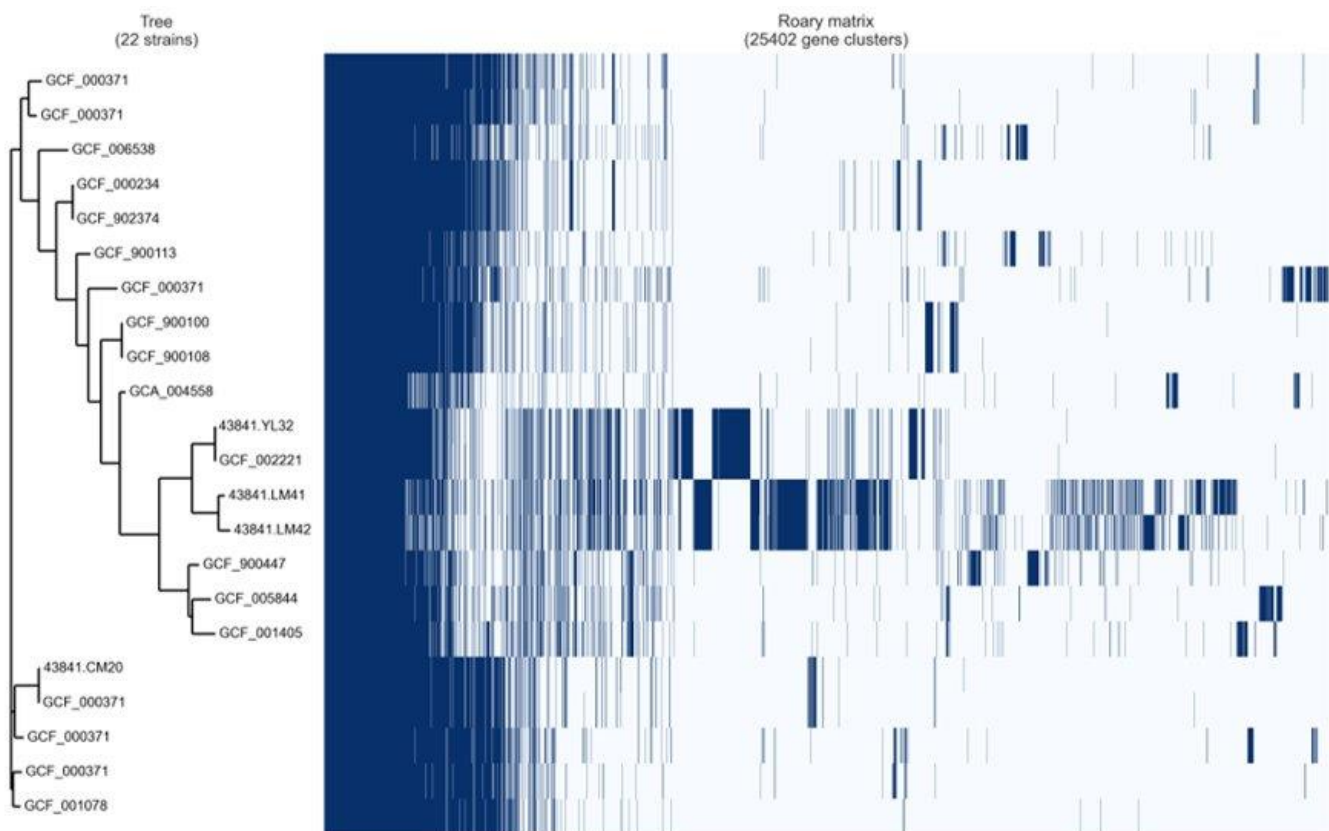
626

627

628

629 **Figure 3**

630 **(a) *C. clostridioforme***



631

632

633

634

635

636

637

638

639

640

641

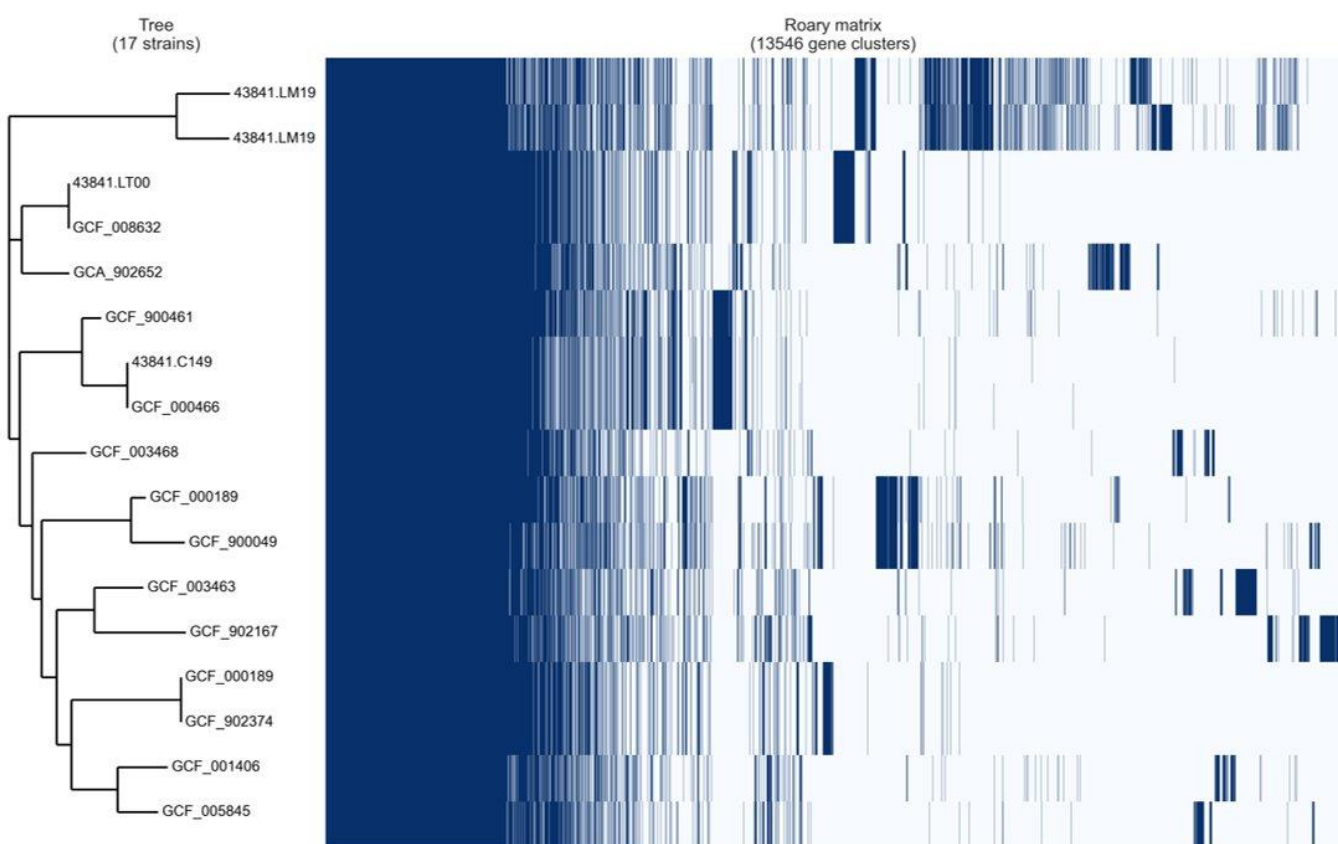
642

643

644

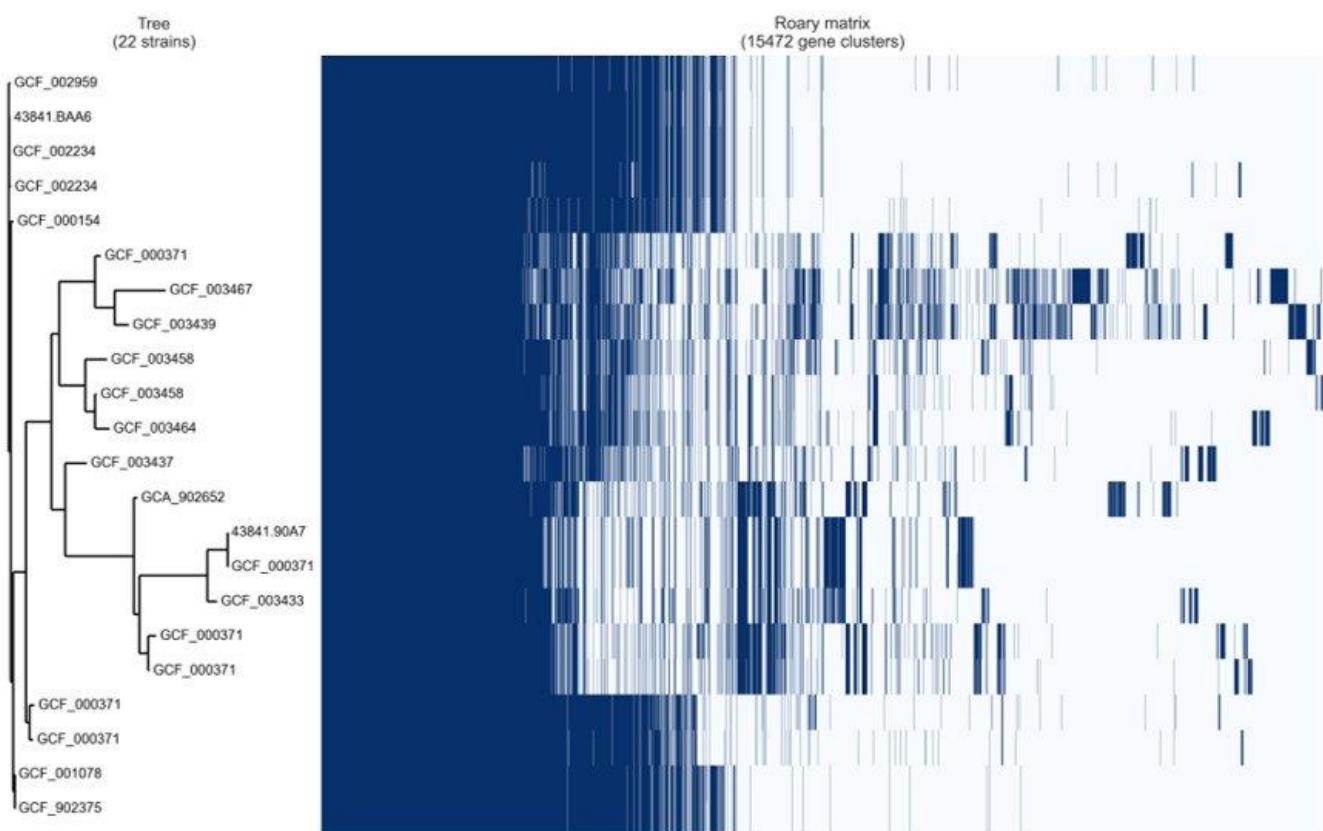
645 (b) *C. symbiosum*

646



661

(c) *C. bolteae*



662

663 **Figure 3: Roary analysis of gene presence/absence in *Clostridium XIVa* species.** Roary
664 analysis of the presence/absence of genes across; (a) 22 strains of *C. clostridioforme*, (b) 17
665 strains of *C. symbiosum* and, (c) 22 strains of *C. bolteae*. New isolates LM41, LM42 and
666 LM19B, LM19R are shown in the *C. clostridioforme* and *C. symbiosum* analysis respectively.

667

668

669

670

671

672

673

674

675

676 **Table 1**

Strain	Genome size (Kbp)	GC skew (%)
<i>C. clostridioforme</i> LM42	7975223	47.84
<i>C. clostridioforme</i> LM41	7977041	47.85
<i>C. clostridioforme</i> YL32	7157460	48.11
<i>C. clostridioforme</i> CM201	5586179	49.16
<i>C. clostridioforme</i> NBRC11352	5687315	48.92
<i>C. clostridioforme</i> 90A8	5974284	48.5
<i>C. clostridioforme</i> 90A1	5806027	48.42
<i>C. clostridioforme</i> CM201	5655915	48.55
<i>C. clostridioforme</i> 90A7	6033914	48.23
<i>C. clostridioforme</i> LT001.00001	5072209	47.89
<i>C. clostridioforme</i> AGR2157	4943165	49.01
<i>C. clostridioforme</i> NCTC11224	5827564	48.97
<i>C. clostridioforme</i> 90A7	6158650	49.22
<i>C. clostridioforme</i> 90A4	5871489	48.15
<i>C. clostridioforme</i> AM07-19	6231573	49.25
<i>C. clostridioforme</i> 1001175	5676948	48.96
<i>C. clostridioforme</i> 90B1	5602152	48.48
<i>C. clostridioforme</i> NLAE-zl-C196	5225716	49.1
<i>C. clostridioforme</i> 2_1_49FAA	5500475	48.53
<i>C. clostridioforme</i> 2789STDY5834865	5514222	49.14
<i>C. clostridioforme</i> 90A3	5549890	48.37
<hr/>		
<i>C. bolteae</i> AM35-14	6793441	48.62
<i>C. bolteae</i> LFYP116	6597056	49.18
<i>C. bolteae</i> 90B8	6482686	48.37
<i>C. bolteae</i> 90B3	6538460	48.94
<i>C. bolteae</i> 90A9	6377378	49.48
<i>C. bolteae</i> OF13-16	6539152	48.65
<i>C. bolteae</i> AF24-13	6422063	48.95
<i>C. bolteae</i> 90B7	6439235	48.78

<i>C. bolteae</i> MGYG-HGUT-01493	6604884	48.89
<i>C. bolteae</i> ATCC BAA-613	6557988	49.05
<i>C. bolteae</i> BAA613.00001	6570176	49.1
<i>C. bolteae</i> TF09-4AC	6232356	49.35
<i>C. bolteae</i> 90A5	6421395	48.87
<i>C. bolteae</i> AF14-18	6430942	49.07
<i>C. bolteae</i> W0P25.026	4404879	50.86
<i>C. bolteae</i> AF27-9	6144412	49.17
<hr/>		
<i>C. symbiosum</i> WAL-14163	5352498	47.36
<i>C. symbiosum</i> LM19R	5298804	47.68
<i>C. symbiosum</i> LM19B	5299950	47.68
<i>C. symbiosum</i> NCTC13233	5054777	47.8
<i>C. symbiosum</i> MGYG-HGUT-001367	4916964	47.59
<i>C. symbiosum</i> ATCC 14940	4823675	47.51
<i>C. symbiosum</i> FYP84	5351947	47.9
<i>C. symbiosum</i> 2789STDY5834864	4727130	47.91
<i>C. symbiosum</i> OF01-1AC	5075475	47.79
<i>C. symbiosum</i> BSD278006168	4763759	47.85
<i>C. symbiosum</i> TS8243C	5266075	47.92
<i>C. symbiosum</i> AM39-1BH	4767382	47.97

677

678 **Table 1: Genome size and GC percentage of *Clostridium XIVa* strains.** Genome size
679 and GC skew of isolated strains *C. clostridioforme* LM41 and LM42, and *C. symbiosum*
680 LM19B and LM19R, in comparison with selected published *C. clostridioforme*, *C. symbiosum*
681 and *C. bolteae* genomes.

682

683

684

685

686

687 **Table 2**

		<i>C. clostridioforme</i>	<i>C. symbiosum</i>	<i>C. bolteae</i>
688	Core genes (99% <= strains <= 100%)	1898	2936	3085
	Soft core genes (95% <= strains < 99%)	920	0	305
	Shell genes (15% <= strains < 95%)	6848	2826	4332
	Cloud genes (0% <= strains < 15%)	12219	5125	7698
	Total genes (0% <= strains <= 100%)	21885	10887	15420

689 **Table 2: Pangenome analysis using Roary of *Clostridium XIVa* species.** Pangenome
690 analysis using Roary of the 55 genomes of *C. clostridioforme*, *C. bolteae* and *C. symbiosum*
691 (excluding W0P9.022) from Figure 2 which had first been annotated using Prokka. Core, soft
692 core, shell, cloud and total genes for each strain are indicated.

693 **Table 3:**

Clostridium clostridioforme

Strain	Number of Phage	Genome size (bp)	Phage bp (kbp)	%Genome = phage
<i>C. clostridioforme</i> LM42	28	7975223	894	12.6249378
<i>C. clostridioforme</i> LM41	29	7977041	878.2	12.3710335
<i>C. clostridioforme</i> YL32	21	7157460	566.8	8.60004916
<i>C. clostridioforme</i> CM201	12	5586179	293.2	5.53941363
<i>C. clostridioforme</i> NBRC11352	14	5687315	294.7	5.46488114
<i>C. clostridioforme</i> 90A8	17	5974284	307.3	5.42263751
<i>C. clostridioforme</i> 90A1	14	5806027	272.5	4.92452644
<i>C. clostridioforme</i> CM201	12	5655915	243.3	4.49505461
<i>C. clostridioforme</i> 90A7	13	6033914	248.7	4.29889024
<i>C. clostridioforme</i> LT001.00001	2	5072209	208.4	4.28470773
<i>C. clostridioforme</i> AGR2157	10	4943165	199.7	4.2100026
<i>C. clostridioforme</i> NCTC11224	11	5827564	228.3	4.07732159
<i>C. clostridioforme</i> 90A7	11	6158650	224.6	3.78493609
<i>C. clostridioforme</i> 90A4	13	5871489	208.1	3.6744783
<i>C. clostridioforme</i> AM07-19	9	6231573	186.3	3.08174668
<i>C. clostridioforme</i> 1001175	6	5676948	167.9	3.04771351
<i>C. clostridioforme</i> 90B1	12	5602152	163.5	3.00625964
<i>C. clostridioforme</i> NLAE-zl-C196	8	5225716	150.9	2.97350682
<i>C. clostridioforme</i> 2_1_49FAA	8	5500475	129.3	2.40729449
<i>C. clostridioforme</i> 2789STDY5834865	8	5514222	124.2	2.30425776
<i>C. clostridioforme</i> 90A3	8	5549890	107.7	1.97898273

Clostridium symbiosum

Strain	Number of Phage	Genome size (bp)	Phage bp (kbp)	%Genome = phage
<i>C. symbiosum</i> WAL-14163	12	5352498	352.4	7.04786186
<i>C. symbiosum</i> LM19R	8	5298804	250.6	4.9641417

<i>C. symbiosum</i> LM19B	8	5299950	250.2	4.95470073
<i>C. symbiosum</i> NCTC13233	0	5054777	153	3.12131702
<i>C. symbiosum</i> MGYG-HGUT-001367	4	4916964	126.8	2.647091
<i>C. symbiosum</i> WAL-14673	4	4916964	126.8	2.647091
<i>C. symbiosum</i> ATCC 14940	4	4823675	106.8	2.26421094
<i>C. symbiosum</i> FYP84	4	5351947	114.8	2.19203318
<i>C. symbiosum</i> 2789STDY5834864	2	4727130	65.6	1.40726328
<i>C. symbiosum</i> OF01-1AC	4	5075475	70.4	1.40657233
<i>C. symbiosum</i> BSD278006168	3	4763759	40.9	0.86600087
<i>C. symbiosum</i> TS8243C	2	5266075	21.3	0.40611847
<i>C. symbiosum</i> AM39-1BH	1	4767382	7.3	0.1533587

Clostridium bolteae

Strain	Number of Phage	Genome size (bp)	Phage bp (kbp)	%Genome = phage
<i>C. bolteae</i> AM35-14	22	6793441	460.1	7.26472805
<i>C. bolteae</i> LFYP116	6	6597056	290.3	4.60300034
<i>C. bolteae</i> 90B8	12	6482686	247.9	3.97607873
<i>C. bolteae</i> 90B3	13	6538460	243.4	3.86652391
<i>C. bolteae</i> 90A9	10	6377378	219.1	3.55781275
<i>C. bolteae</i> OF13-16	11	6539152	223.9	3.54538505
<i>C. bolteae</i> AF24-13	8	6422063	194.5	3.12321208
<i>C. bolteae</i> 90B7	8	6439235	185.9	2.97281371
<i>C. bolteae</i> WAL-14578	7	6604884	180.7	2.8128086
<i>C. bolteae</i> ATCC BAA-613	7	6557988	175.8	2.75454123
<i>C. bolteae</i> BAA613.00001	7	6570176	172	2.68826616
<i>C. bolteae</i> TF09-4AC	5	6232356	143	2.34835999
<i>C. bolteae</i> 90A5	6	6421395	145.9	2.3249162
<i>C. bolteae</i> AF14-18	6	6430942	113.7	1.79983607
<i>C. bolteae</i> W0P25.026	1	4404879	20.4	0.46527763
<i>C. bolteae</i> AF27-9	1	6144412	10.4	0.16954646

695 **Table 3: Putative phage content of *Clostridium* XIVa species.** Analysis of the putative
696 phage content of the genomes of listed *Clostridium* XIVa species using Phaster. The number
697 of phage, total genome size, putative phage material detected, and the percentage of the
698 total genome occupied by this phage material is indicated.

699

700

701

702

703

704

705

706

707

708

709

710

711

712

713

714

715

716

717

718

719

720

721

722

723 **Table 4:** IMEs and ICEs

Clostridium symbiosum LM19B

Name	Location	Length/bp	Type
Region1	177767..254712	76946	Putative ICE with T4SS
Region2	2298904..2328641	29738	Putative IME
Region3	4467243..4543305	76063	Putative ICE with T4SS

Clostridium symbiosum LM19R

Name	Location	Length/bp	Type
Region1	890897..977449	86553	Putative ICE with T4SS
Region2	1881404..1911154	29751	Putative IME
Region3	2874565..2965979	91415	Putative ICE with T4SS
Region4	3082855..3135714	52860	Putative ICE with T4SS
Region5	4627784..4655274	27491	Putative IME
Region6	5230762..5235310	4549	Putative IME without identified DR

Clostridium clostridioforme LM41

Name	Location	Length/bp	Type
Region1	531191..724491	193301	Putative ICE with T4SS
Region2	1197371..1199761	2391	Putative IME without identified DR
Region3	2041831..2195442	153612	Putative ICE with T4SS
Region4	2336403..2354509	18107	Putative IME without identified DR
Region5	2623858..2640032	16175	Putative IME
Region6	3029722..3033702	3981	Putative IME without identified DR
Region7	3193104..3340431	147328	Putative ICE with T4SS
Region8	3731406..3818133	86728	Putative ICE with T4SS
Region9	4910211..4945863	35653	Putative ICE with T4SS
Region10	5423367..5478842	55476	Putative AICE with Rep and Tra
Region11	5947737..6062237	114501	Putative ICE with T4SS
Region12	7206164..7398777	192614	Putative ICE with T4SS
Region13	7835678..7848309	12632	Putative IME

Clostridium clostridioforme LM42

Name	Location	Length/bp	Type
Region1	530235..641955	111721	Putative ICE with T4SS
Region2	1089702..1133607	43906	Putative IME without identified DR
Region3	1695836..1717892	22057	Putative IME without identified DR
Region4	1945247..2001257	56011	Putative ICE with T4SS
Region5	2441505..2448548	7044	Putative IME without identified DR
Region6	2586949..2658045	71097	Putative ICE with T4SS
Region7	2892979..2914638	21660	Putative ICE with T4SS
Region8	3167058..3186257	19200	Putative IME without identified DR
Region9	3512594..3525203	12610	Putative IME

Region10	3891579..3924258	32680	Putative IME
Region11	4552655..4651363	98709	Putative ICE with T4SS
Region12	4874134..4938049	63916	Putative ICE with T4SS
Region13	5264895..5487459	222565	Putative ICE with T4SS
Region14	5648469..5652450	3982	Putative IME without identified DR
Region15	6051571..6091699	40129	Putative IME
Region16	6398610..6425203	26594	Putative IME
Region17	7221062..7303454	82393	Putative ICE with T4SS

724

725 **Table 4: Putative integrative conjugative elements (ICEs) and integrative mobile**
726 **elements (IMEs) detected in *Clostridium symbiosum* LM19B and LM19 R and**
727 ***Clostridium clostridioforme* strains LM41 and LM42.** Identification of putative ICEs and
728 IMEs in each strain was carried out using ICEfinder (Add ref). ICEs were detected with and
729 without type 4 secretion systems (T4SS) while IMEs were examined for presence of direct
730 repeats (DR).

731

732

733

734

735

736

737

738

739

740

741

742

743

744

745

746

Table 5: antiSmash analysis of *Clostridium XIVa* genomes*C. clostridioforme*

Strain	BGCs	Putative metabolite(s)
YL32	13	cyclic-lactone-autoinducer (x8), ranthipeptide, transAT-PKS, NRPS, Tyrosine recombinase XerC, ranthipeptide, NRPS
LM41	10	NRPS-like (x2), transAT-PKS, lanthipeptide-class-ii, cyclic-lactone-autoinducer (x4), NRPS (butyrolactone related), ranthipeptide
LM42	10	NRPS-like (x2), transAT-PKS, lanthipeptide-class-ii, cyclic-lactone-autoinducer (x4), NRPS (butyrolactone related), ranthipeptide
GCF_900113155.1_IMG-taxon_2593339147	5	ranthipeptide, cyclic-lactone-autoinduce, NRPS-like (x3)
GCF_005844705.1_ASM584470v1	4	ranthipeptide, NRPS-like, cyclic-lactone-autoinducer, butyrolactone
GCF_006538465.1_ASM653846v1_	3	cyclic-lactone-autoinducer, ranthipeptide, NRPS
GCF_000371505.1_Clos_clos_90A8_V1	3	cyclic-lactone-autoinducer, ranthipeptide, RRE-containing
43841.BAA613.1_	2	NRPS-like, ranthipeptide
43841.CM201.1	2	cyclic-lactone-autoinducer, ranthipeptide
GCF_000234155.1_Clos_clos_2_1_49FAA_V1	2	cyclic-lactone-autoinducer, ranthipeptide
GCF_000371545.1_Clos_clos_90A6_V	2	cyclic-lactone-autoinducer, ranthipeptide
GCF_000371565.1_Clos_clos_90A4_V1	2	cyclic-lactone-autoinducer, ranthipeptide
GCF_000371585.1_Clos_clos_90A3	2	cyclic-lactone-autoinducer, ranthipeptide
GCF_000371585.1_Clos_clos_90A3_V	2	cyclic-lactone-autoinducer, ranthipeptide
GCF_000424325.1_ASM42432v1	2	cyclic-lactone-autoinducer, ranthipeptide
GCF_001078445.1_Clos_clos_WAL_7855_v11	2	ranthipeptide, NRPS-like
GCF_003467855.1_ASM346785v1	2	ranthipeptide, NRPS-like
GCF_900100685.1_IMG-taxon_2654588145	2	ranthipeptide, NRPS-like
GCF_902374585.1_MGYG-HGUT-01386	2	cyclic-lactone-autoinducer, ranthipeptide
GCF_900100685.1	2	cyclic-lactone-autoinducer, ranthipeptide
GCF_900108895.1_IMG-taxon_2654588144	2	cyclic-lactone-autoinducer, ranthipeptide
GCF_900447015.1_57530_A01	2	ranthipeptide, NRPS-like
GCF_000371485.1_Clos_clos_90B1_V1	2	cyclic-lactone-autoinducer, ranthipeptide
GCF_001405335.1_13470_2_84	1	ranthipeptide

GCF_000371525.1_Clos_clos_90A7_V1	1	ranthipeptide
43841.90A7.1_	1	ranthipeptide
43841.C14940.1	1	ranthipeptide
GCF_003433765.1_ASM343376v1	1	ranthipeptide

C. symbiosum

GCA_902652275.1_CsymbiosumLFYP84	2	ranthipeptide, NRPS
GCF_000189595.1_Clos_symb_WAL_14163_V1	1	ranthipeptide
GCF_000189615.1_Clos_symb_WAL_14673_V2	1	ranthipeptide
52421E_LM19B	1	ranthipeptide
52422E_LM19R	1	ranthipeptide
GCF_003463485.1_ASM346348v1	1	ranthipeptide
GCF_001406475.1_13470_2_83_	1	ranthipeptide
GCF_008632235.1_ASM863223v1	1	ranthipeptide
GCF_900049235.1	1	ranthipeptide
GCF_003468225.1_ASM346822v1	1	ranthipeptide
GCF_900461275.1_51765_A02	1	ranthipeptide
GCF_902167935.1_TS_8243C_mod2_	1	ranthipeptide
CF_902374315.1_MGYG-HGUT-01367	1	ranthipeptide
GCF_005845085.1_ASM584508v1	1	ranthipeptide

C. bolteae

GCF_003464745.1_ASM346474v1	3	cyclic-lactone-autoinducer, rantipeptide, NRPS-like
GCA_004555815.1_ASM455581v1	3	phosphonate, NRPS-like, ranthipeptide
GCA_004558155.1_ASM455815v1	2	ranthipeptide, cyclic-lactone-autoinducer
GCF_000154365.1_ASM15436v1	2	ranthipeptide, NRPS-like
GCF_000371645.1_Clos_bolt_90B8_V1_	2	ranthipeptide, NRPS-like
GCF_000371665.1_Clos_bolt_90B7_V1	2	ranthipeptide, NRPS-like
GCF_000371725.1_Clos_bolt_90A5_V1	2	ranthipeptide, NRPS-like
GCF_002234575.1_ASM223457v1	2	ranthipeptide, NRPS-like

GCF_002959675.1_ASM295967v1	2	ranthipeptide, NRPS-like
GCF_003439835.1_ASM343983v1	2	ranthipeptide, NRPS-like
GCF_003458165.1_ASM345816v1	2	ranthipeptide, NRPS-like
GCF_003458625.1_ASM345862v1	2	ranthipeptide, NRPS-like
GCF_902375545.1_MGYG-HGUT-01493	2	ranthipeptide, NRPS-like
GCA_902652185.1_CbolteaeLFYP116	1	ranthipeptide
GCF_000371705.1_Clos_bolt_90A9_V1	1	ranthipeptide
GCF_003437595.1_ASM343759v1	1	ranthipeptide

748 **Table 5: Putative secondary metabolite producing regions in *Clostridium XIV* species.** antiSMASH analysis indicating that as well as
 749 having larger genomes, *C. clostridioforme* strains LM41 and LM42 contain, alongside strain *C. clostridioforme* YL32, increased numbers of
 750 BGCs indicating increased capability to make secondary metabolites. While these strains had either 10 or 13 BGCs each the majority of other
 751 strains, including *C. symbiosum* LM19B and LM19R carried a single BGC for a putative ranthipeptide.

752 **Supplementary Figures**

753 **Supplementary Figure 1: R plots of Roary analysis of *C. clostridioforme*.** Roary plots
754 showing the number of; new genes, conserved genes, number of genes in the pan genome,
755 unique genes, BlastP hits with a different percentage, conserved versus total genes, and new
756 versus unique genes when compared across the cluster.

757

758 **Supplementary Figure 2: R plots of Roary analysis of *C. symbiosum*.** Roary plots showing
759 the number of; new genes, conserved genes, number of genes in the pan genome, unique
760 genes, BlastP hits with a different percentage, conserved versus total genes, and new versus
761 unique genes when compared across the cluster.

762

763 **Supplementary Figure 3: R plots of Roary analysis of *C. bolteae*.** Roary plots showing the
764 number of; new genes, conserved genes, number of genes in the pan genome, unique genes,
765 BlastP hits with a different percentage, conserved versus total genes, and new versus unique
766 genes when compared across the cluster.

767

768

769

770

771

772

773

774

775

776

777

778

779

780 **Supplementary Table 1**

Most Common Phage	Region LM41A	Region LM42D	Length
PHAGE_Bacill_BM5_NC_029069(2)	209674-225678	2373988-2389992	16Kb
PHAGE_Clostr_vB_CpeS_CP51_NC_021325(11)	300120-332811	2464434-2497125	32.6Kb
PHAGE_Bacter_Lily_NC_028841(16)	1065870-1120786	3230180-3285096	54.9Kb
PHAGE_Stx2_c_1717_NC_011357(2)	1446706-1455307	3611016-3619617	8.6Kb
PHAGE_Mycoba_Toto_NC_028906(1)	1518051-1529355	3682361-3693665	11.3Kb
PHAGE_Cellul_phi4:1_NC_021788(1)	1761998-1768494	3926308-3932804	6.4Kb
PHAGE_Stx2_c_1717_NC_011357(2)	2353117-2374256	4517427-4538566	21.1Kb
PHAGE_Faecal_FP_Mushu_NC_047913(6)	2377933-2389186	4542243-4553496	11.2Kb
PHAGE_Geobac_E2_NC_009552(7)	3073910-3107688	5238226-5272004	33.7Kb
PHAGE_Brevib_Jenst_NC_028805(1)	3263800-3282793	5428114-5447107	18.9Kb
PHAGE_Stx2_c_1717_NC_011357(2)	3355805-3368955	5520119-5533269	13.1Kb
PHAGE_Lactob_Ld3_NC_025421(6)	3444120-3496219	5608432-5660531	52.1Kb
PHAGE_Faecal_FP_Brigit_NC_047909(16)	3833804-3901899	5996298-6064396	68Kb
PHAGE_Aeriba_AP45_NC_048651(3)	4036975-4063629	6199472-6226126	26.6Kb
PHAGE_Faecal_FP_Epona_NC_047910(18)	4122091-4147409	6284588-6309906	25.3Kb
PHAGE_Escher_SH2026Stx1_NC_049919(2)	6436617-6449560	6982158-6995101	12.9Kb
PHAGE_Coryne_Lederberg_NC_048790(6)	6639228-6672036	6759682-6792490	32.8Kb
PHAGE_Faecal_FP_Mushu_NC_047913(7)	6674387-6696127	6735590-6757321	21.7Kb
PHAGE_Faecal_FP_Mushu_NC_047913(28)	6704568-6769447	6662270-6727149	64.8Kb
PHAGE_Stx2_c_1717_NC_011357(2)	6871307-6880236	6551481-6560410	8.9Kb
PHAGE_Faecal_FP_Lagaffe_NC_047911(2)	7469934-7505967	1849601-1885634	36Kb
PHAGE_Clostr_phiMMP03_NC_028959(12)	7486703-7607995	1866370-1987662	121.2Kb
PHAGE_Stx2_c_1717_NC_011357(2)	124672-133277	101331-109936	8.6Kb
PHAGE_Butyri_Arawn_NC_048848(3)	1274694-1312803		38.1Kb
PHAGE_Brevib_Abouo_NC_029029(2)	1290856-1329164		38.3Kb
PHAGE_Bacill_Mgbh1_NC_041879(1)	4536044-4558405		22.3Kb
PHAGE_Butyri_Arawn_NC_048848(7)	5193058-5225315		32.2Kb
PHAGE_Bacill_vB_BceS_MY192_NC_048633(2)	5707065-5723538		16.4Kb
PHAGE_EnterophiFL4A_NC_013644(4)	6182332-6206543		24.2Kb
PHAGE_Butyri_Arawn_NC_048848(7)		421970-455831	33.8Kb
PHAGE_Staphy_StB20_NC_019915(1)		1086849-1120221	33.3Kb
PHAGE_Bacill_BM5_NC_029069(3)		3437170-3493729	56.5Kb
PHAGE_Clostr_phiCT453A_NC_028991(4)		7201748-7242355	40.6Kb
PHAGE_Bacill_vB_BceS_MY192_NC_048633(2)		7697257-7720384	23.1Kb

781

782 **Supplementary Table 1: Phage carriage by *C. clostridioforme* strains LM41 and LM42.**

783 Analysis of phage carriage by Phaster of *C. clostridioforme* strains LM41 and LM42 indicated
784 while many phage regions were common to both strains, each had 5-6 putative phage regions
785 absent in the other strain.

786

787